Neuron
Article

V1 and V2b Interneurons Secure the Alternating Flexor-Extensor Motor Activity Mice Require for Limbed Locomotion

Jingming Zhang,[1,6] Guillermo M. Lanuza,[1,2,6] Olivier Britz,[1] Zhi Wang,[3] Valerie C. Siembab,[4] Ying Zhang,[1,7] Tomoko Velasquez,[1] Francisco J. Alvarez,[4,5] Eric Frank,[3] and Martyn Goulding[1,*]
[1]Molecular Neurobiology Laboratory, The Salk Institute for Biological Studies, La Jolla, CA 92037, USA
[2]Fundación Instituto Leloir, IIBBA-CONICET, Buenos Aires 1405, Argentina
[3]Department of Molecular Physiology and Pharmacology, Tufts University School of Medicine, Boston, MA 02111, USA
[4]Department of Neurosciences, Cell Biology, and Physiology, Wright State University, Dayton, OH 45435, USA
[5]Department of Physiology, Emory University, Atlanta, GA 30322, USA
[6]Co-first author
[7]Present address: Department of Anatomy and Neurobiology, Dalhousie University, Halifax, NS B3H 4R2, Canada
*Correspondence: goulding@salk.edu
http://dx.doi.org/10.1016/j.neuron.2014.02.013

SUMMARY

Reciprocal activation of flexor and extensor muscles constitutes the fundamental mechanism that tetrapod vertebrates use for locomotion and limb-driven reflex behaviors. This aspect of motor coordination is controlled by inhibitory neurons in the spinal cord; however, the identity of the spinal interneurons that serve this function is not known. Here, we show that the production of an alternating flexor-extensor motor rhythm depends on the composite activities of two classes of ventrally located inhibitory neurons, V1 and V2b interneurons (INs). Abrogating V1 and V2b IN-derived neurotransmission in the isolated spinal cord results in a synchronous pattern of L2 flexor-related and L5 extensor-related locomotor activity. Mice lacking V1 and V2b inhibition are unable to articulate their limb joints and display marked deficits in limb-driven reflex movements. Taken together, these findings identify V1- and V2b-derived neurons as the core interneuronal components of the limb central pattern generator (CPG) that coordinate flexor-extensor motor activity.

INTRODUCTION

Terrestrial vertebrates use their limbs for a range of motor tasks, from simple protective reflexes and locomotion to more complex volitional movements, such as reaching, grasping, and grooming. These motor behaviors require the production of a reciprocating pattern of motor impulses to antagonist groups of flexor and extensor muscles (Sherrington, 1893; Grillner, 1975). Multiple studies have shown that flexor-extensor alternation is an intrinsic property of the locomotor central pattern generator (CPG) in limbed animals (Brown, 1911; Eccles et al., 1956; Goulding, 2009; Grillner, 1975; Grillner and Jessell, 2009; Kiehn, 2006; Ladle et al., 2007). However, efforts to identify the interneuron (IN) cell types that secure flexor-extensor alternation have met with limited success, and because of this we still know very little about the overall organization of the locomotor CPG in limbed vertebrates.

Prior efforts to interrogate the structure of the neural networks that control flexor-extensor alternation have shown that the flexor-extensor control system is composed of inhibitory neurons that reside in each half of the spinal cord (Cowley and Schmidt, 1995; Sernagor et al., 1995; Talpalar et al., 2011; Whelan et al., 2000). A major drawback of the pharmacological approaches used in these studies is the widespread inactivation of inhibitory neurons regardless of their subtype or connectivity (Cowley and Schmidt, 1995; Bracci et al., 1996; Kremer and Lev-Tov, 1997; Cazalets et al., 1998). This has precluded a more detailed determination of the neuronal cell types limbed animals use to produce an alternating flexor-extensor motor rhythm. More recently, genetic approaches in mice that selectively inactivate or delete specific interneuron classes have been employed to determine the contribution molecularly defined classes of INs make to locomotion (Crone et al., 2008; Gosgnach et al., 2006; Lanuza et al., 2004; Zhang et al., 2008; Zagoraiou et al., 2009). Whereas these functional studies have identified neurons with selective roles in regulating left-right coordination, rhythmogenesis, and the speed of the step cycle, the cells that are responsible for establishing an alternating flexor-extensor rhythm have still not been isolated (Goulding, 2009; Grillner and Jessell, 2009; Kiehn, 2006; Stepien and Arber, 2008).

Initial attempts to determine the molecular identity and developmental provenance of the spinal INs that establish the alternating flexor-extensor motor activity mice use for limb movements focused on V1 INs. V1 INs are a class of ipsilaterally projecting inhibitory neurons (Betley et al., 2009; Sapir et al., 2004; Saueressig et al., 1999) that includes cells possessing the anatomical features of reciprocal Ia inhibitory interneurons (IaINs; Alvarez et al., 2005), a cell type thought to play a prominent role in flexor-extensor inhibition (Eccles et al., 1956; Feldman and Orlovsky, 1975). However, spinal cords

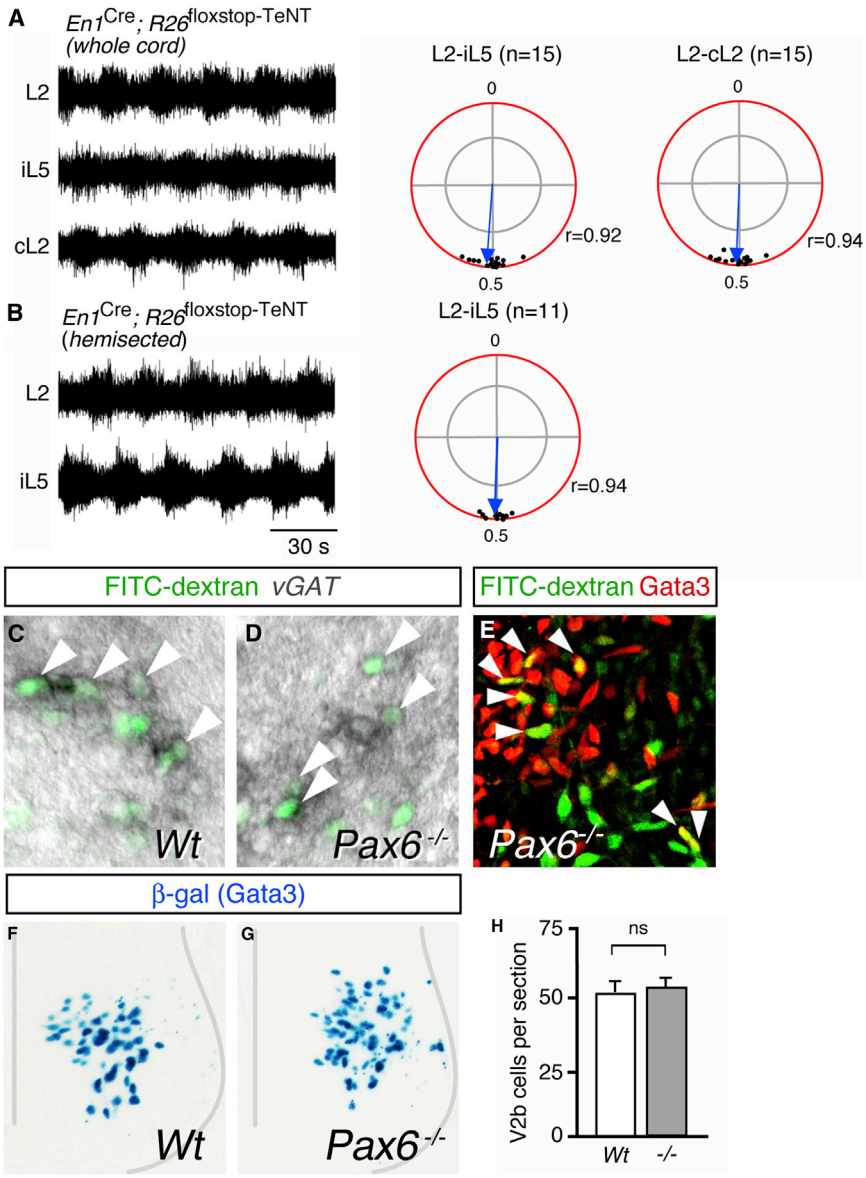

Figure 1. A Non-V1 IN Population Is Involved in Securing Reciprocal Flexor-Extensor Activity

(A and B) Left: Representative extracellular recordings from ventral roots of a P0 *En1*^{Cre}; *R26*$^{floxstop\text{-}TeNT}$ spinal cord showing locomotor ENG activity prior to and after hemisection. Signals were recorded from the L2, iL5, and cL2 ventral roots. Right: Circular plots showing averaged L2-iL5 phase relationships in whole (upper) and hemisected (lower) preparations. Inner circle indicates an r significance value of p = 0.01. Points located near 0.5 represent alternation. Alternating L2-iL5 locomotor activity is maintained before and after hemisection. The L2-cL2 phase relationship is also shown. The number of cords analyzed is indicated (n).

(C and D) Representative sections of FITC-dextran-injected spinal cords from wild-type and *Pax6*$^{-/-}$ embryos at E18.5, showing FITC-dextran^{+} cells rostral and ipsilateral to the application site. *vGAT* in situ hybridization identifies a subset of FITC-dextran^{+} cells as inhibitory neurons in wild-type and *Pax6*$^{-/-}$ spinal cords (arrowheads).

(E) A section from an FITC-dextran-labeled E18.5 *Pax6*$^{-/-}$ embryo showing FITC-dextran^{+}/Gata3^{+} cells (yellow, arrowheads).

(F–H) Comparison of Gata3^{+} V2b cell numbers in E11.5 *Gata3*^{lacZ} and *Gata3*^{lacZ}; *Pax6*$^{-/-}$ spinal cords as assessed by β-galactosidase staining. Quantification is shown in (H) (mean ± SEM; n = 12 sections, three cords for each sample).

lacking V1 INs retain reciprocal Ia inhibition (Wang et al., 2008), and they produce an alternating pattern of flexor-extensor locomotor activity (Gosgnach et al., 2006). We now show that V2b INs cooperate with V1 INs to secure the alternating pattern of flexor-extensor motor activity that is necessary for limbed locomotion. We also find that cells with the characteristic properties of IaINs develop from both V1 and V2b INs. Taken together, our results demonstrate that flexor-extensor control is a distributed property of the walking CPG shared by V1 and V2b IN cell types. Interestingly, V1 and V2b INs share a common phylogenetic heritage with two classes of inhibitory neurons in the spinal cords of aquatic vertebrates. This suggests that the neurons walking vertebrates employ for flexor-extensor control were originally part of the swimming CPG and were recruited for this new function during the course of evolution.

RESULTS

A Population of Non-V1 INs Secure Alternating Flexor-Extensor Activity

As a first step toward defining the cellular organization of the circuits that secure flexor-extensor alternation in mice, we examined the pattern of motor activity in hemisected spinal cords lacking V1 IN-derived inhibition. Severing all commissural connections in the *En1*^{Cre}; *R26*$^{floxstop\text{-}TeNT}$ spinal cord produced a strictly reciprocating L2 (flexor-related) and iL5 (ipsilateral extensor-related) motor rhythm (Figure 1B; n = 11 hemicords) when locomotor-like activity was induced with N-methyl-D aspartic acid (NMDA) and 5-hydroxytryptamine (5-HT). This pattern of L2-iL5 activity was similar to that seen in the intact *En1*^{Cre}; *R26*$^{floxstop\text{-}TeNT}$ spinal cord (Figure 1A) and in the *Pax6*$^{-/-}$ spinal cord (Figure S1 available online). Moreover, it suggests that other ipsilateral inhibitory neurons in the spinal cord secure flexor-extensor alternation, either alone or in combination with V1 INs.

Retrograde dextran tracing experiments with fluorescein isothiocyanate (FITC)-dextran were then used to search for ipsilaterally projecting inhibitory neurons in the ventral spinal cord of *Pax6*$^{-/-}$ mice that lack V1 INs (Ericson et al., 1997; Gosgnach et al., 2006). In E18.5 *Pax6*$^{-/-}$ spinal cords, we

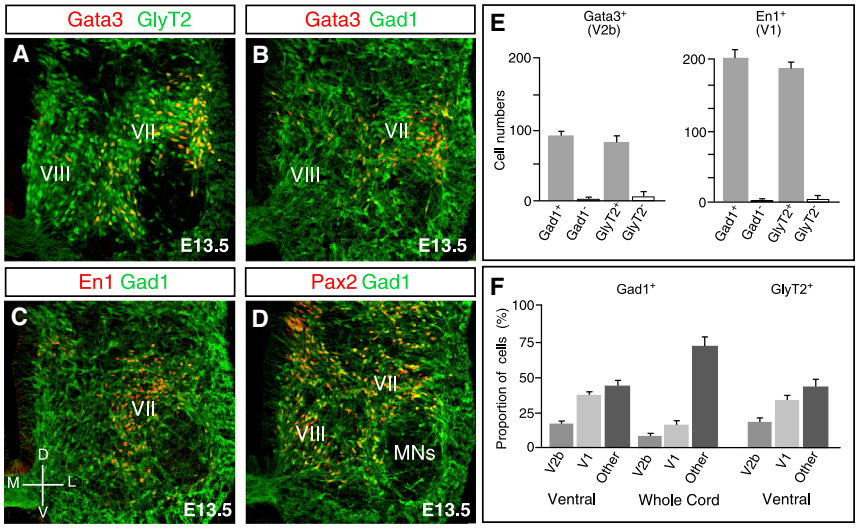

Figure 2. Neurotransmitter Phenotype and Axonal Projections of V2b INs

(A and B) Gata3 expression in the spinal cords of *GlyT2-GFP* (A) and *Gad1-GFP* (B) transgenic mice at E13.5.

(C) Coexpression of En1 and Gad1.

(D) Coexpression of Pax2 and Gad1.

(E) Quantification of Gata3 and En1 coexpression with Gad1 and GlyT2. Bars indicate the number of cells per 30 μm hemicord cross-section (mean ± SEM, n = 3 cords).

(F) Quantification of the proportion of Gad1$^+$ and GlyT2$^+$ neurons that are either V1 or V2b INs at E13.5.

detected ipsilaterally projecting neurons that express the inhibitory vesicular amino acid transporter *vGAT* (*Slc32a1*) (Figure 1D). Many of these cells were located rostral to the injection site (Figure 1E). In view of prior studies showing that V2b INs are inhibitory (Al-Mosawie et al., 2007; Lundfald et al., 2007), a *Gata3*^{lacZ} knockin allele (van Doorninck et al., 1999) was used to test whether the *Pax6*$^{-/-}$ cord contains a normal complement of V2b INs. No difference was detected in the number of differentiating V2b INs in age-matched E11.5 embryos (Figures 1F–1H; wild-type 52 ± 4 cells versus *Pax6*$^{-/-}$ 57 ± 3 cells per section), thereby raising the possibility that V2b INs secure flexor-extensor alternation in the *Pax6*$^{-/-}$ cord in the absence of V1 INs.

Characterization of the V2b INs

We then mapped the distribution and number of Gata3$^+$ V2b INs in spinal cords of *GlyT2-GFP* (Zeilhofer et al., 2005) and *Gad1-GFP* (Tamamaki et al., 2003) transgenic mice. These analyses were performed at E13.5, as Gad1-GFP is strongly downregulated in the ventral horn at later developmental times. Localization of Gata3 and GlyT2-GFP at E13.5 revealed that >90% of Gata3$^+$ neurons coexpress GFP (Figures 2A and 2E). A slightly higher number of Gata3$^+$ V2b INs (~95%) expressed GFP in E13.5 *Gad1-GFP* reporter mice (Figures 2B and 2E). Cell counts revealed that Gata3$^+$ V2b INs constitute ~19% of the Gad1-GFP$^+$ cells in the ventral half of the spinal cord and 9% of the Gad1-GFP$^+$ cells in the whole cord at E13.5 (Figure 2F). By comparison V1 INs account for ~37% of the ventral inhibitory neurons and 17% of the inhibitory neurons in the whole cord (Figures 2C and 2F).

The medial ventral horn (lamina VIII) was largely devoid of V2b and V1 INs (Figures 2A–2D), which is consistent with previous studies showing lamina VIII is primarily comprised of commissural IN cell types (Harrison et al., 1986; Stepien et al., 2010). These include Gad1-GFP$^+$/Pax2$^+$ cells (Figure 2D) that are likely to be V0 INs and dI6 INs (Andersson et al., 2012; Lanuza et al., 2004). Although the majority of ipsilaterally projecting inhibitory INs in lamina VII (~85%) are V1 and V2b INs, these two classes only account for approximately 30%–35% of the ipsilaterally projecting inhibitory neurons in the spinal cord as a whole. The majority of Gad1-GFP$^+$ neurons (~56%) in the E13.5 spinal cord are derived from dorsal Lbx1$^+$neurons, which are for the most part, ipsilaterally projecting dI4 and dIL$_A$ INs (Gross et al., 2002).

To assess the potential contribution that V2b INs make to flexor-extensor motor control, we asked whether motor neurons innervating the hindlimb musculature receive inhibitory synaptic inputs from V2b INs. To this end, a *Gata3*^{Cre} knockin allele was generated (Figure S2) and crossed with a Cre-conditional *Thy1::floxstop-YFP* reporter (Buffelli et al., 2003) to indelibly mark the V2b INs and their axons. V2b INs are primarily located in lamina VII and have processes that extend throughout the ventral horn (Figures 3A and 3F). In order to assess the number and distribution of V2b inhibitory synaptic contacts on hindlimb motor neurons, Cy5-conjugated Cholera Toxin-B (CTB) was injected into single hindlimb muscles in *Gata3*^{Cre}; *Thy1::floxstop-YFP* mice (Figure 3B). Sections through the lumbar spinal cords of these CTB-labeled mice at P15 revealed numerous vGAT$^+$/GlyT2$^+$ presynaptic contacts on motor neurons within the iliopsoas (IP), gluteus (GL), quadriceps (Q), and posterior biceps-semitendinosus (PB/St) motor pools (Figures 3C and 3E). Motor neurons innervating the gastrocnemius and tibialis anterior muscles were also decorated with V2b inhibitory contacts (data not shown). V2b inhibitory contacts were found on the soma of cholinergic V0c INs and on other neurons in lamina VII and VIII, many of which are likely to be premotor CPG neurons (Figure 3D).

Further analysis of V2b-derived and non-V2b-derived inhibitory contacts onto the soma of CTB-labeled hindlimb motor neurons revealed that the proportion of V2b-derived vGAT$^+$/GlyT2$^+$ inhibitory contacts versus all vGAT$^+$/GlyT2$^+$ contacts varies in a motor-pool-specific manner (Figure 3E), from 23% (IP motor neurons) to 41% (GL motor neurons). V2b INs are therefore a significant source of the inhibition to hindlimb motor neurons. A similar analysis of V1 IN-derived contacts (Figure 3E) revealed that 38%–59% of the inhibitory synaptic contacts on the soma of hindlimb motor neurons are derived from V1 INs (Figure 3E). Of these, one-third of the contacts can be attributed to Renshaw cell inputs (Figure 3E), which like Ia IN synapses are primarily located on the soma and proximal dendrites of motor

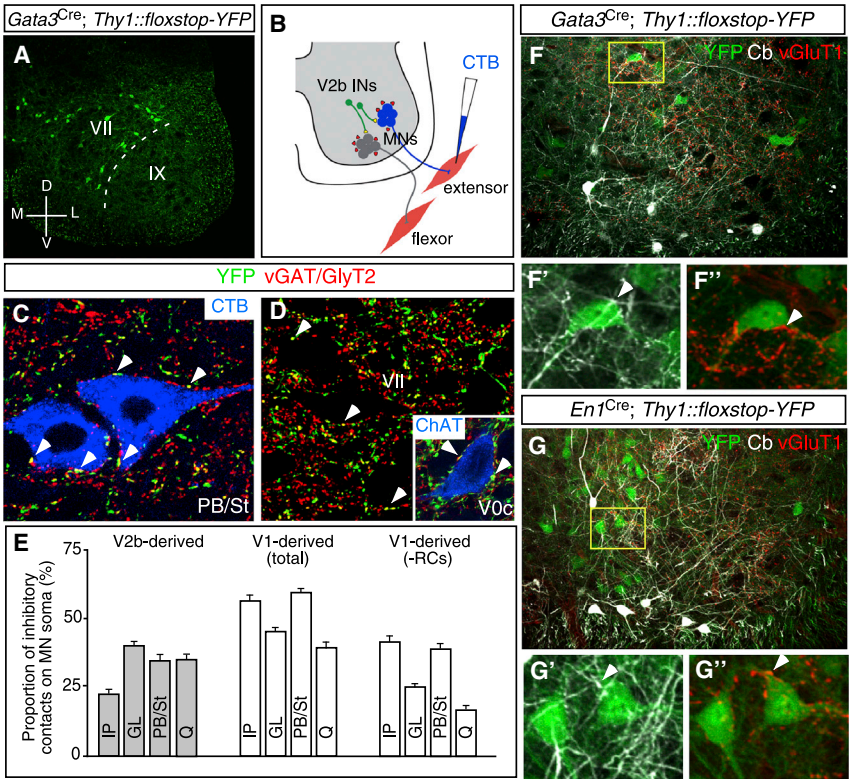

Figure 3. IaINs Are Derived from V1 and V2b INs

(A) P15 *Gata3*^{Cre}; *Thy1::floxstop-YFP* spinal cord showing V2b INs are located predominantly in lamina VII. Note the V2b cells close to the border of lamina VII/IX.

(B) Schematic showing the protocol for CTB labeling of specific hindlimb motor neuron pools and visualization of inhibitory synaptic contacts.

(C) Section showing the soma and proximal dendrites of two motor neurons (blue) labeled by injecting Cy5-CTB into the PB/St muscles. GlyT2^{+}/vGAT^{+} inhibitory synaptic contacts from V2b INs are indicated (arrowheads).

(D) Section showing V2b IN-derived GlyT2^{+}/vGAT^{+} inhibitory contacts (arrowheads) on the soma of lamina VII neurons. Inset: Inhibitory contacts (arrowheads) from V2b INs on a ChAT^{+} V0c IN (blue).

(E) Quantification of V1- and V2b-derived synaptic contacts on iliopsoas (IP), gluteus (GL), posterior biceps-semitendinous (PB/St), and quadriceps (Q) motor neurons (mean ± SEM, n = 15 cells per motor pool).

(F and G) Sections through the lumbar spinal cord of P15 *Gata3*^{Cre}; *Thy1::floxstop-YFP* (F), and *En1*^{Cre}; *Thy1::floxstop-YFP* (G) mice, showing neurons with the anatomical features of IaINs. Cells decorated with calbindin^{+} (Cb^{+}) (F' and G') and vGluT1^{+} (F'' and G'') contacts were scored as IaINs. Cell counts for V2b-derived IaINs and V1-derived IaINs are given in Table S1.

neurons (Jankowska, 1992). Interestingly, the relative proportion of V1 and V2b inhibitory contacts onto hindlimb motor neurons matches the ~2-fold difference in V1 versus V2b cell numbers in the lumbar cord (95 ± 14 V1 cells versus 42 ± 10 V2b cells per ventral horn section). These analyses point to V1 and V2b INs being the primary source of inhibition to the somatic compartment of hindlimb motor neurons. They are also consistent with the idea that the V2b IN population may include IaINs. Unfortunately, we were unable to determine the number and relative abundance of V1- and V2b-derived synaptic contacts on the dendrites of these motor neurons due to the limitations of the CTB labeling technique.

Our observation that a subpopulation of V2b INs are located close to the border with lamina IX (Figure 3A), where IaINs in the cat spinal cord are found (Jankowska and Lindström, 1972) coupled with the persistence of Ia inhibition in mice lacking V1 INs (Wang et al., 2008), prompted us to ask if the V2b INs might be a source of IaINs. To this end, *Gata3*^{Cre}; *Thy1::floxstop-YFP* reporter mice were used to search for V2b INs that possess the immunohistochemical features of IaINs. *En1*^{Cre}; *Thy1::floxstop-YFP* mice were also used to identify and analyze putative V1-derived IaINs. Cells were scored as IaINs on the basis of high-density convergent inputs from calbindin^{+} Renshaw cell axons and vGluT1^{+} primary sensory afferents (Alvarez et al., 2005). Approximately 19% of the V2b INs and 29% of the V1 INs in the lumbar spinal cord were categorized as IaINs using these criteria. These numbers are likely underestimates, as some IaINs may receive vGluT1 inputs on more distal dendrites that could not be scored in this study. Our findings reveal that cells bearing the anatomical characteristics of IaINs develop from two distinct inhibitory neuron lineages.

Inactivating V2b IN Transmission Compromises Flexor-Extensor Coordination

To determine the functional contribution that V2b INs make to motor coordination and flexor-extensor alternation, we crossed the *Gata3*^{Cre} knockin allele (Figure S2) with a conditional TeNT allele (*R26*$^{floxstop\text{-}TeNT}$; Zhang et al., 2008), so as to abrogate inhibitory transmission in all V2b-derived INs. As expected, wild-type spinal cords produced a strong locomotor-like rhythm in which L2-iL5 ventral root activity was strictly out of phase (Figure 4A). This alternating L2-iL5 activity is widely considered to be a proxy measure of flexor-extensor activity (Kiehn, 2006). *Gata3*^{Cre}; *R26*$^{floxstop\text{-}TeNT}$ cords also displayed a predominantly alternating pattern of L2 and iL5 ventral root activity, although the phasing of this activity was more variable than that seen in wild-type spinal cords (Figure 4B). This suggests that L2-iL5 coordination is mildly degraded in cords lacking V2b-derived inhibition. Nonetheless, the overall phase relationship between L2 and iL5 in the *Gata3*^{Cre}; *R26*$^{floxstop\text{-}TeNT}$ cord remains alternating rather than synchronous. Abrogating V2b transmission had no effect on left-right alternation between opposing L2 ventral roots (Figure 4B).

We then asked whether the CPG network that generates L2-iL5 alternation is fully functional in hemisected spinal cords, where V2b-derived inhibition is disrupted. Whereas wild-type (Figure 4C) and *En1*^{Cre}; *R26*$^{floxstop\text{-}TeNT}$ (Figure 1B) hemicords exhibited an invariant reciprocating pattern of L2-iL5 activity,

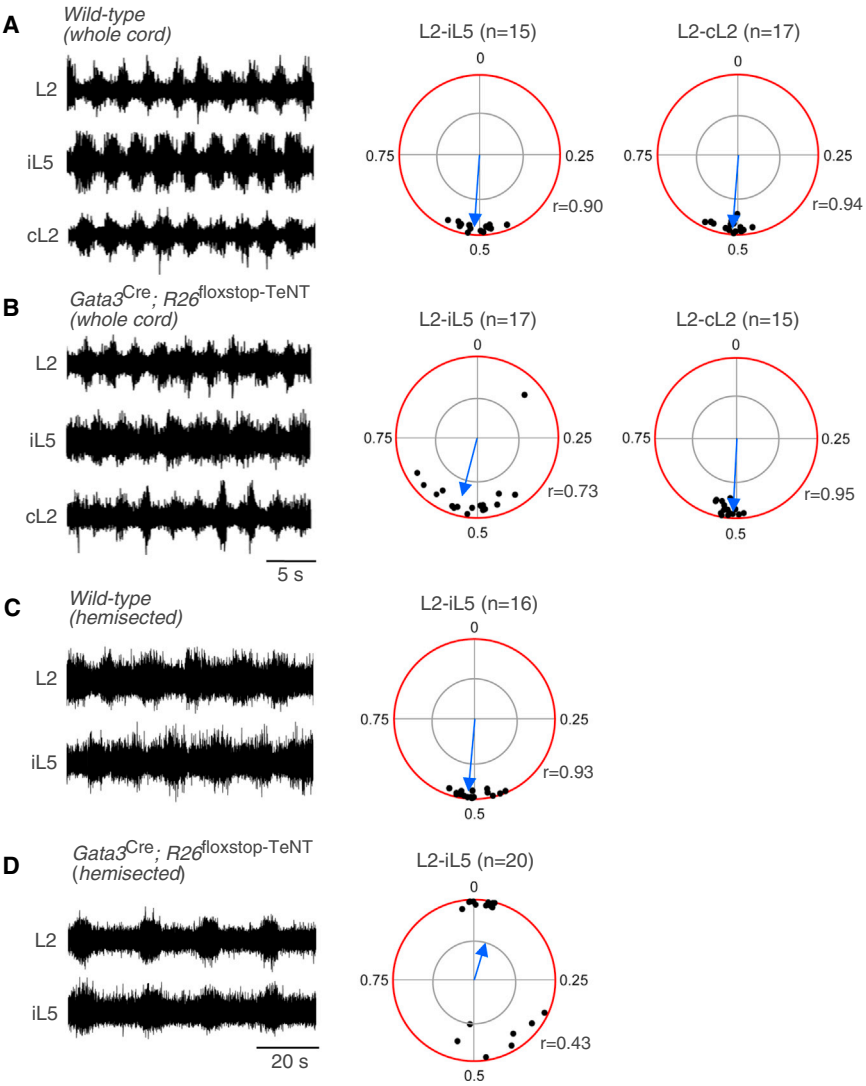

Figure 4. Abolishing V2b IN Transmission Degrades Flexor-Extensor Coordination

(A and B) Left: extracellular recordings from L2, iL5, and cL2 ventral roots of wild-type and *Gata3*^{Cre}; *R26*$^{floxstop\text{-}TeNT}$ from P0 whole cords following the induction of locomotor activity with 5 μM NMDA and 15 μM 5-HT. Right: circular plots showing the phase of bursts in iL5 and cL2 with respect to L2. Each point in the circular plot represents the average phase for one spinal cord (25–50 steps). The angular vector (arrow) and r-value (r) for each genotype represents the mean phase relationship for all recorded cords (n). The inner circle indicates an r significance value of p = 0.01. Alternating flexor-extensor (L2-iL5) activity is observed in wild-type (A) whole cords and in all but one *Gata3*^{Cre}; *R26*$^{floxstop\text{-}TeNT}$ (B) whole cord.

(C and D) Left: locomotor-activity following spinal cord hemisection. Left: the normal pattern of flexor-extensor (L2-iL5) alternation in wild-type hemisected cords (C) is markedly reduced in *Gata3*^{Cre}; *R26*$^{floxstop\text{-}TeNT}$ hemisected cords (D), with 13/20 cords displaying synchronous L2-iL5 activity. Right: circular plots showing the L2-iL5 phase vector points and r-values for the cords in each experimental group. n, number of cords analyzed for each group.

the majority of *Gata3*^{Cre}; *R26*$^{floxstop\text{-}TeNT}$ hemicords displayed synchronous L2-iL5 activity (Figure 4D). Thirteen of twenty *Gata3*^{Cre}; *R26*$^{floxstop\text{-}TeNT}$ hemicords had mean L2-iL5 vector points close to 0, which indicates synchronous L2-iL5 activity. There were, however, some *Gata3*^{Cre}; *R26*$^{floxstop\text{-}TeNT}$ hemicords (n = 7/20) that retained a loosely alternating pattern of L2-iL5 activity. This suggests that other ipsilateral inhibitory neurons secure flexor-extensor alternation in the absence of V2b-derived inhibition. The observation that hemisected *Gata3*^{Cre}; *En1*^{Cre}; *R26*$^{floxstop\text{-}TeNT}$ cords generate a synchronous pattern of L2-iL5 activity (Figure S3) suggests these cells may be V1 INs.

Inactivation of V2b and V1 INs Abrogates Reciprocal Flexor-Extensor Motor Activity

Our discovery that L2-iL5 coordination is degraded upon abrogating V2b functionality prompted us to test whether V2b and V1 INs act in a cooperative manner to generate an alternating flexor-extensor motor rhythm. *Gata3*^{Cre}; *En1*^{Cre}; *R26*$^{floxstop\text{-}TeNT}$ mice induced to locomote with NMDA and 5-HT displayed a strictly synchronous pattern of flexor-extensor motor activity (Figure 5A; n = 14/14 cords). Electrically stimulating sacral sensory afferents also produced a synchronous pattern of L2-iL5 locomotor activity in all *Gata3*^{Cre}; *En1*^{Cre}; *R26*$^{floxstop\text{-}TeNT}$ cords tested (Figure 5C; n = 8/8 cords). By contrast, L2-iL5 activity was always alternating in electrically stimulated wild-type cords (Figure 5B; n = 7/7 cords). All *Gata3*^{Cre}; *En1*^{Cre}; *R26*$^{floxstop\text{-}TeNT}$ cords displayed a strictly alternating activity pattern in the contralateral roots (Figures 5A and 5C). Taken together, these findings show that V1 and V2b INs play an essential role in controlling the phasing of L2-iL5 activity but do not contribute to left-right alternation.

Altering the Balance of Excitatory and Inhibitory Transmission Fails to Rescue Alternation in the *Gata3*^{Cre}; *En1*^{Cre}; *R26*$^{floxstop\text{-}TeNT}$ Cord

To rule out the possibility that the synchronous L2-iL5 activity we observe in the *Gata3*^{Cre}; *En1*^{Cre}; *R26*$^{floxstop\text{-}TeNT}$ cord might be due to a change in the balance between excitation and inhibition within the locomotor network, we asked if flexor-extensor alternation is rescued when excitatory transmission is decreased or inhibitory transmission is enhanced in the *Gata3*^{Cre}; *En1*^{Cre}; *R26*$^{floxstop\text{-}TeNT}$ cord. Excitatory transmission was either attenuated by reducing the concentration of NMDA in the perfusate or by adding a low concentration of 6-cyano-7-nitroquinoxaline-2,3-dione (CNQX) to the perfusate to weaken non-NMDA

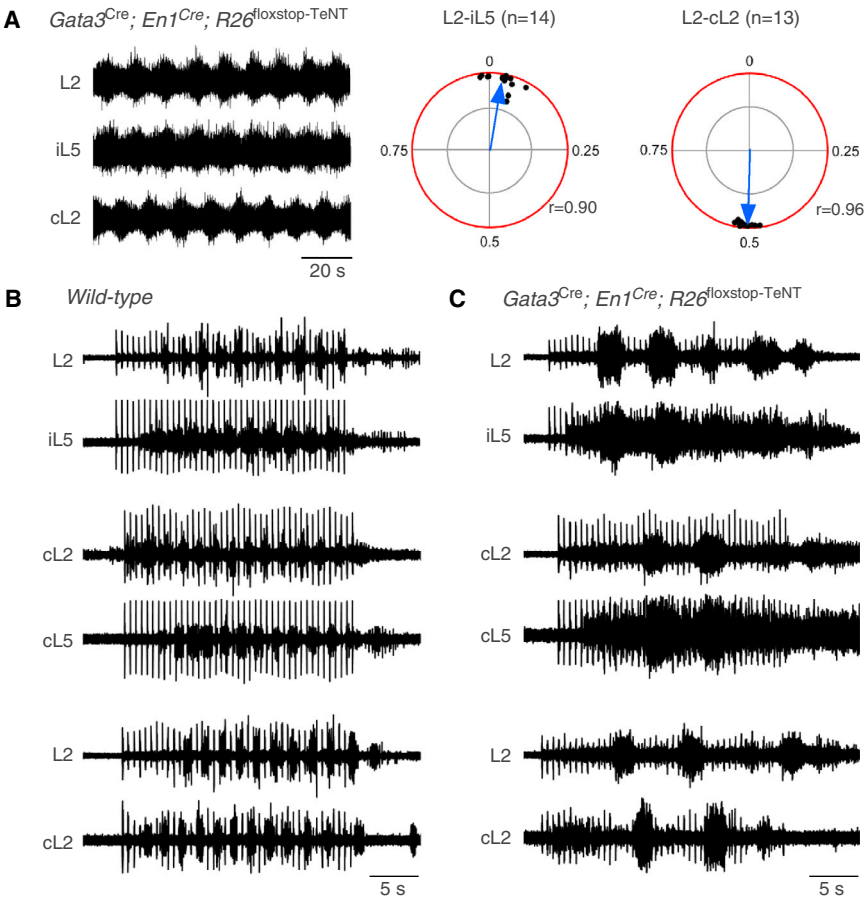

Figure 5. V1 and V2b INs Function Cooperatively to Establish Flexor-Extensor Alternation

(A) Left: example of extracellular recordings from L2, iL5, and cL2 ventral roots of a P0 *Gata3*^{Cre}; *En1*^{Cre}; *R26*$^{floxstop\text{-}TeNT}$ spinal cord following application of 5 μM NMDA and 15 μM 5-HT. Right: phase relationship between L2 and iL5 (L2-iL5) and between L2 and cL2 (L2-cL2) ventral roots. The inner circle indicates an r significance value of p = 0.01.

(B and C) Extracellular recordings from L2, iL5, and cL2 ventral roots of P0 wild-type (B) and P0 *Gata3*^{Cre}; *En1*^{Cre}; *R26*$^{floxstop\text{-}TeNT}$ (C) spinal cords following sacral dorsal root stimulation. Normal flexor-extensor (L2-iL5) and left-right (L2-cL2) alternation is observed in wild-type cords (B). Flexor-extensor (L2-iL5) alternation is absent in *Gata3*^{Cre}; *En1*^{Cre}; *R26*$^{floxstop\text{-}TeNT}$ cords; however, left-right (L2-cL2) alternation remains intact. n, number of cords analyzed.

excitatory transmission, which is the major source of excitatory drive to the locomotor CPG (Cowley et al., 2005; Whelan et al., 2000). When excitation was decreased by either method, L2-iL5 ventral root activity remained synchronous (Figures 6A–6C). In a second series of experiments, sarcosine was added to the perfusate to enhance glycinergic transmission. This treatment also failed to restore alternating L2-iL5 activity in the *Gata3*^{Cre}; *En1*^{Cre}; *R26*$^{floxstop\text{-}TeNT}$ cord (Figure 6D), as did the addition of nipecotic acid (Figure S4). Left-right alternation was preserved following all of these manipulations, thus providing further evidence that V1- and V2b-derived inhibition has a selective role in securing flexor-extensor coordination. By contrast, blocking all inhibitory transmission in the spinal cord produced an abnormal pattern of motor activity in which all lumbar ventral roots were synchronously active (Figure S4). This pattern of activity was highly irregular rather than rhythmic, suggesting that it does not represent normal locomotor activity. Taken together, these data argue that differences in the balance of excitation and inhibition are unlikely to account for the loss of flexor-extensor alternation in the *Gata3*^{Cre}; *En1*^{Cre}; *R26*$^{floxstop\text{-}TeNT}$ cord.

Newborn Mice Lacking V1 and V2b Inhibitory Transmission Are Unable to Move Their Limbs

To confirm that the loss of alternating L2-iL5 activity seen in vitro represents an absence of reciprocating flexor-extensor activity in the hindlimb CPG, we examined the motor activity that is produced in antagonist Q and PB muscles following drug-induced locomotion. As inactivating the V1 and/or V2b INs with TeNT results in early neonatal lethality, these analyses were performed at P0. Electromyographic (EMG) recordings made from P0 wild-type animals using a limbs-attached spinal cord preparation (Pearson et al., 2003) revealed a strictly alternating pattern of Q-PB activity, as expected (Figure 7A; n = 6/6 mice). By contrast, *Gata3*^{Cre}; *En1*^{Cre}; *R26*$^{floxstop\text{-}TeNT}$ newborn mice displayed rhythmic coactivation of both muscle groups (Figure 7B; n = 7/7mice).

In addition to the loss of flexor-extensor coordination that occurs during fictive locomotion, distinct differences were noted in the motor behaviors of newborn *Gata3*^{Cre}; *En1*^{Cre}; *R26*$^{floxstop\text{-}TeNT}$ mice. Whereas P0 wild-type pups displayed spontaneous bouts of air stepping in which they extended and flexed their limbs, P0 *Gata3*^{Cre}; *En1*^{Cre}; *R26*$^{floxstop\text{-}TeNT}$ pups displayed no such movements. Instead, all four limbs were completely immobilized.

Further behavioral testing of the *Gata3*^{Cre}; *En1*^{Cre}; *R26*$^{floxstop\text{-}TeNT}$ pups revealed clear deficits in a range of motor reflexes, including the righting response that requires a sequence of flexion and extension movements by all four limbs. Whereas newborn wild-type pups displayed a strong righting response when placed on their backs (n = 6 mice, three trials each), *Gata3*^{Cre}; *En1*^{Cre}; *R26*$^{floxstop\text{-}TeNT}$ pups were never able to fully rotate from a supine to prone position (n = 6 mice, three trials each). Occasionally, *Gata3*^{Cre}; *En1*^{Cre}; *R26*$^{floxstop\text{-}TeNT}$ pups were able to place both front feet on the ground, although the time to do so was >18 s for the *Gata3*^{Cre}; *En1*^{Cre}; *R26*$^{floxstop\text{-}TeNT}$ pups as compared to <5 s for wild-type pups. There was no measureable difference in the righting time for *En1*^{Cre}; *R26*$^{floxstop\text{-}TeNT}$ and *Gata3*^{Cre}; *R26*$^{floxstop\text{-}TeNT}$ pups compared to wild-type pups.

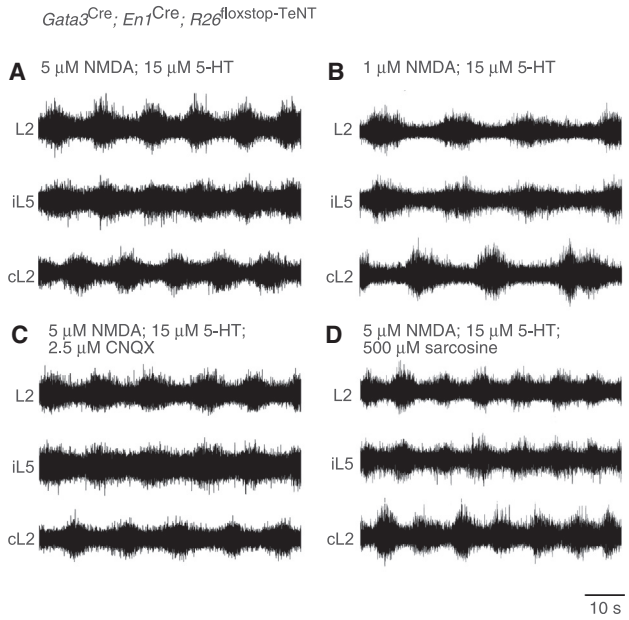

Figure 6. Loss of Flexor-Extensor Alternation in *Gata3*^{Cre}; *En1*^{Cre}; *R26*$^{floxstop\text{-}TeNT}$ Spinal Cords Is Not due to Changes in the Balance of Excitation and Inhibition

(A) Extracellular recordings from the L2, iL5, and cL2 ventral roots of *Gata3*^{Cre}; *En1*^{Cre}; *R26*$^{floxstop\text{-}TeNT}$ whole-cord preparations at P0 after induction of locomotor activity with 5 μM NMDA and 15 μM 5-HT.

(B and C) Synchronous flexor-extensor (L2-iL5) activity is maintained at lower NMDA concentrations (B) and after reducing AMPA-dependent excitatory transmission with 2.5 μM CNQX (C).

(D) Enhancing inhibitory transmission with the glycine uptake inhibitor sarcosine (500 μM) does not rescue L2-iL5 alternation. Note that left-right (L2-cL2) alternation is preserved under all conditions.

The response of newborn pups to tail pinch was also examined. Newborn mice normally respond to a single tail pinch by flexing and extending their hindlimbs (Figures 7C and 7E). This sequence of limb movements was observed in wild-type, *En1*^{Cre}; *R26*$^{floxstop\text{-}TeNT}$ and *Gata3*^{Cre}; *R26*$^{floxstop\text{-}TeNT}$ pups (Figure 7E; n = 43 mice) but never in *Gata3*^{Cre}; *En1*^{Cre}; *R26*$^{floxstop\text{-}TeNT}$ pups (Figures 7D and 7E; n = 10 mice). *Gata3*^{Cre}; *En1*^{Cre}; *R26*$^{floxstop\text{-}TeNT}$ pups did however produce marked lateral bending movements of the torso (Figure S5), indicating the sensory reflex pathways for sensing noxious stimuli are still intact in these animals. These behavioral tests, together with the in vitro spinal cord analyses, demonstrate that mice lose their ability to execute flexor-extensor-driven limb movements when V1 and V2b inhibitory transmission is abolished.

Abolition of Reciprocal Inhibitory Reflexes in Mice Lacking V1 and V2b INs

To further understand the nature of the loss of alternating flexor-extensor activity in the *Gata3*^{Cre}; *En1*^{Cre}; *R26*$^{floxstop\text{-}TeNT}$ mice, we asked whether these animals retain the inhibitory reflex pathway between the quadriceps nerve and PB/St motor neurons (Figure 8A; Wang et al., 2008) that is used as a measure of IaIN-mediated reciprocal inhibition in the cat (Hultborn et al., 1971; Jankowska and Roberts, 1972). In newborn wild-type pups (n = 8 mice), inhibitory potentials with synaptic latencies of 13–17 ms were recorded in 23 of 29 motor neurons, which we know from our previous analysis are likely to be disynaptic (Wang et al., 2008). All 23 potentials with a disynaptic latency were hyperpolarizing when the cell was first impaled, demonstrating that these potentials are inhibitory. During the recording, hyperpolarizing potentials gradually became depolarizing as the resting potential of the cell became more negative (Figure 8; see also Wang et al., 2008). To confirm that these potentials are inhibitory, we performed an additional test on some of these motor neurons. Short positive current pulses (80–150 pA) were injected to depolarize the membrane potential by 35–50 mV and test if the depolarizing currents were converted to hyperpolarizing potentials. In eight motor neurons from four mice tested in this manner, positive current injection converted depolarizing disynaptic potentials to hyperpolarizing potentials (Figure 8B).

This same pathway was examined in P0 *Gata3*^{Cre}; *En1*^{Cre}; *R26*$^{floxstop\text{-}TeNT}$ pups (n = 5 animals), where only 7 of 20 motor neurons displayed potentials consistent with a disynaptic latency ($\leq$16.5 ms). These potentials remained depolarizing, and none were reversed upon positive current injection (Figures 8C and 8F; n = 7/7 motor neurons). Thus, while some *Gata3*^{Cre}; *En1*^{Cre}; *R26*$^{floxstop\text{-}TeNT}$ mice still possess disynaptic afferent inputs to motor neurons, the inputs are not inhibitory. Interestingly, long-latency inhibitory potentials (>18 ms) were observed in many PB/St motor neurons (see Figures 8D and 8E), demonstrating inhibitory inputs to PB/St motor neurons are not entirely eliminated when V1 and V2b transmission is abrogated. Finally, eliminating either V1- or V2b-derived inhibitory transmission alone failed to abolish inhibitory potentials in PB/St motor neurons that fall within the disynaptic latency window (Figure S6; Wang et al., 2008). These findings show that the V1 and V2b IN classes both contribute to reciprocal inhibition in the spinal cord, and together with the anatomical analysis in Figure 3, they demonstrate a clear dichotomy in the developmental origin of IaINs.

DISCUSSION

V1 and V2b INs constitute the core elements of a distributed inhibitory network that secures the reciprocal pattern of flexor and extensor motor activity that mice use for limb-driven movements. This finding is also consistent with our discovery that IaINs are derived from V1 and V2b IN progenitors. Our results suggest that V1 and V2b INs are largely responsible for this facet of motor coordination, as the inactivation of other inhibitory neuron populations, including V0 INs and Lbx1-derived inhibitory neuron cell types, does not alter flexor-extensor phasing (Lanuza et al., 2004; Talpalar et al., 2013; M.G., unpublished data). Although flexor-extensor coordination appears to be a primary function of the V1 and V2b INs, we cannot rule out additional roles for V1 and V2b INs in motor behaviors that cannot be assessed in the isolated spinal cord preparation.

This study, together with previous studies (Whelan et al., 2000; Kiehn, 2006), argues that commissural neurons do not contribute directly to the control of flexor-extensor alternation, as the rodent

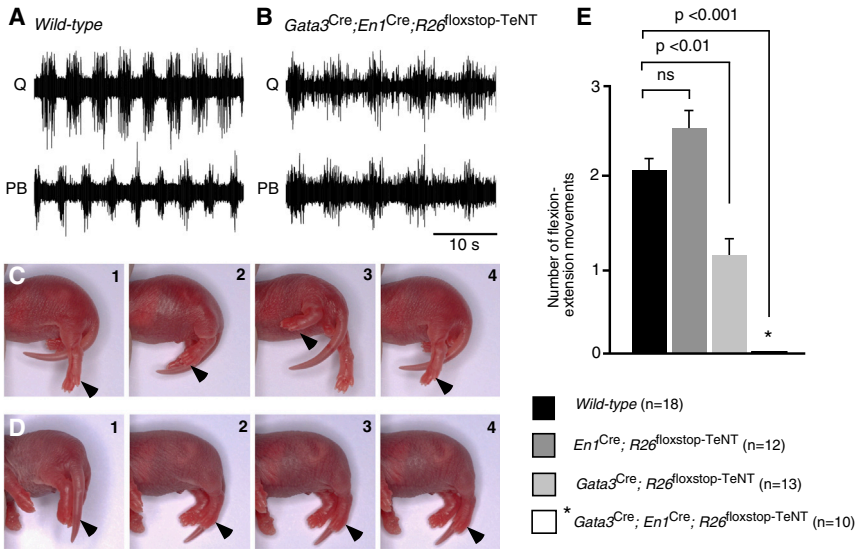

Figure 7. Defective Limb Movement in Newborn *Gata3*^{Cre}; *En1*^{Cre}; *R26*$^{floxstop\text{-}TeNT}$ Mice

(A and B) EMG recordings from knee extensor (quadriceps, Q) and knee flexor (posterior biceps, PB) muscles of newborn P0 mice following induction of locomotor activity in a limbs-attached spinal cord preparation with a cocktail of 10 μM NMDA, 25 μM 5-HT, and 25 μM dopamine. Quadriceps (Q) and posterior biceps (PB) muscle activity is alternating in wild-type animals (A) and synchronous in *Gata3*^{Cre}; *En1*^{Cre}; *R26*$^{floxstop\text{-}TeNT}$ mice (B).

(C) A series of time-lapse images of P0 wild-type pups showing flexion-extension movements of the hindlimbs in response to tail pinch.

(D) *Gata3*^{Cre}; *En1*^{Cre}; *R26*$^{floxstop\text{-}TeNT}$ mutant animals show no flexion-extension movements, and their limbs are immobile.

(E) Number of flexion-extension movements in response to a single tail pinch in wild-type pups and age-matched *En1*^{Cre}; *R26*$^{floxstop\text{-}TeNT}$, *Gata3*^{Cre}; *R26*$^{floxstop\text{-}TeNT}$ and *Gata3*^{Cre}; *En1*^{Cre}; *R26*$^{floxstop\text{-}TeNT}$ animals. Student's t test. Error bars, SEM.

spinal CPG still produces a reciprocating pattern of L2-iL5 flexor-extensor activity when all commissural connections are severed. Interestingly, the degradation of flexor-extensor alternation is more pronounced in the hemisected *Gata3*^{Cre}; *R26*$^{floxstop\text{-}TeNT}$ cord compared to the intact *Gata3*^{Cre}; *R26*$^{floxstop\text{-}TeNT}$ cord. This raises the possibility that some commissural INs provide excitatory drive to V1 INs. V1-derived IaINs are contacted by glutamatergic V3 INs (Zhang et al., 2008), raising the possibility that V3 commissural INs subserve this function.

Contribution of V1 and V2b IN Inputs to Motor Neuron Inhibition

The high density of V1 and V2b inhibitory contacts on the soma and proximal dendrites of motor neurons suggests that V1 and V2b INs provide most of the inhibition to the soma of these cells (Figure 3). They are therefore likely to strongly gate excitatory inputs to motor neurons. Other studies show inhibitory commissural INs (Kiehn, 2006; Lanuza et al., 2004) and inhibitory INs in the dorsal horn (Jankowska, 1992; Tripodi et al., 2011; Wilson et al., 2010) also synapse with motor neurons. The location of these synapses is not known, and a significant fraction of these may be on motor neuron dendrites (see Ornung et al., 1998; Shigenaga et al., 2005). Given our current inability to score inhibitory contacts on dendrites, the relative contribution that commissural INs, dorsal inhibitory INs, and V1/V2b INs make to motor neuron inhibition remains to be determined. Nonetheless, our demonstration that V1 and V2b INs are strictly required for flexor-extensor alternation (see Figures 5 and 7), coupled with the abundance of V1 and V2b IN inputs on motor neuron soma, suggests that the actions of these other inhibitory cell types on flexion-extension movements are likely to be highly dependent on V1 and V2b INs. It should also be noted that V1 and V2b INs provide inhibitory inputs to other CPG neurons (Figure 3), including excitatory neurons that are also likely to play an important role in shaping flexor-extensor activity (Figure 9).

Role of Inhibition in Establishing Flexor-Extensor Alternation

Prior studies demonstrating flexor-extensor alternation is only abrogated upon blocking all inhibitory transmission in the cord have led to speculation that the relative level of inhibition versus excitation in the spinal motor network may be the mechanism that generates an alternating flexor-extensor motor output from the walking CPG. Our data argue against this possibility, as pharmacological manipulations that reduce excitation in the *Gata3*^{Cre}; *En1*^{Cre}; *R26*$^{floxstop\text{-}TeNT}$ cord spinal cord, while changing the amplitude and frequency of the motor rhythm, do not alter the phasing of L2-iL5 flexor-extensor-related activity (Figure 6). Furthermore, the motor pattern that emerges when bicuculline and strychnine are used to block inhibitory transmission differs in two key aspects from the pattern observed following V1 and V2b IN inactivation. First, widespread pharmacological blockade of glycinergic and GABAergic neurotransmission results in irregular episodes of high-amplitude motor neuron bursting interspersed with periods of little of no activity (Figure S4). The periodicity of these bursts is highly variable, arguing that this activity is not rhythmic. Second, in contrast to the *Gata3*^{Cre}; *En1*^{Cre}; *R26*$^{floxstop\text{-}TeNT}$ cord, where left-right alternation is preserved (Figures 4 and 5), abrogating inhibition causes all the lumbar ventral roots to burst synchronously (Figure S4; see also Cowley and Schmidt, 1995; Kremer and Lev-Tov, 1997).

Functional Organization of the Walking CPG

This study demonstrates two important principles about the cellular organization of the walking CPG. First, flexor-extensor activity is not controlled by a single class of neurons but is instead encoded by the composite actions of V1 and V2b INs. This suggests that the evolutionary transition from a swimming circuit to a walking circuit was not accomplished by simply adding a new cell type with a dedicated role in flexor-extensor control. Second, it shows V1 and V2b INs are not part of the

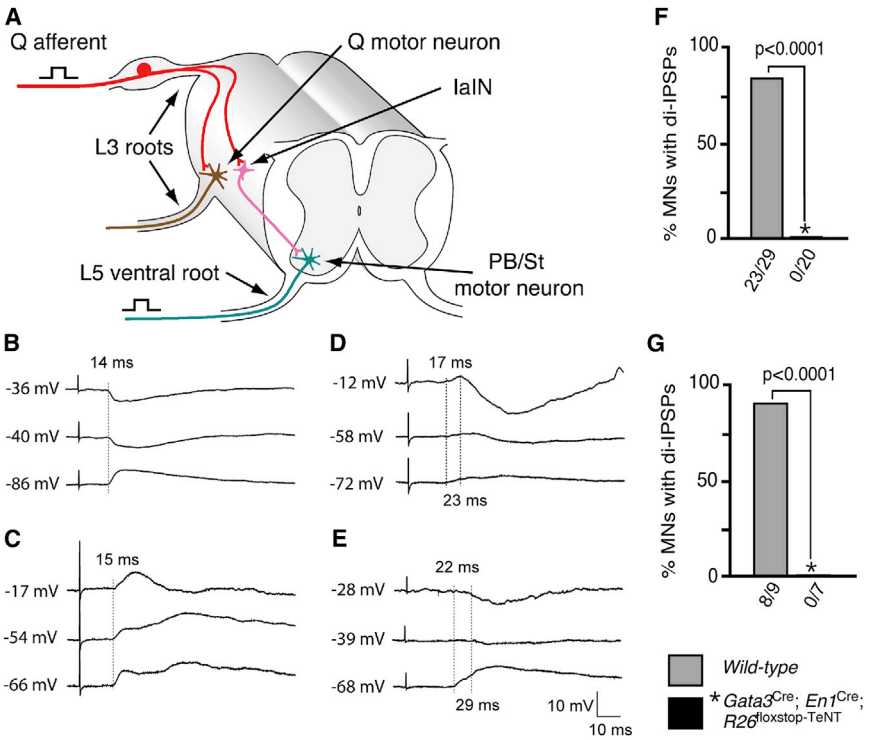

Figure 8. Loss of Reciprocal Inhibitory Reflexes in Mice Lacking V1 and V2b INs

(A) Schematic showing disynaptic pathway from quadriceps (Q) afferent nerve to posterior biceps-semitendinosus (PB/St) motor neurons.

(B–E) Intracellular recordings of synaptic responses in PB/St motor neurons were elicited by stimulating the Q nerve (3–5× threshold). Hyperpolarizing inhibitory potentials often become depolarizing as the resting potential (indicated at the beginning of each trace) increased. An inhibitory potential (IPSP) in a wild-type mouse that is disynaptic (13–17 ms) is shown in (B). In *Gata3*^{Cre}; *En1*^{Cre}; *R26*$^{floxstop\text{-}TeNT}$ mice, synaptic potentials with disynaptic latencies (13–17 ms) either were depolarizing and could not be reversed with current injection (C) or were long latency (D and E). A hyperpolarizing response (23 ms) that is inconsistent with disynaptic inhibition is shown in (E).

(F and G) Frequency of disynaptic inhibitory potentials in control and *Gata3*^{Cre}; *En1*^{Cre}; *R26*$^{floxstop\text{-}TeNT}$ pups before (F) and after (G) current injection. The significance between the number of disynaptic IPSPs in wild-type versus *Gata3*^{Cre}; *En1*^{Cre}; *R26*$^{floxstop\text{-}TeNT}$ samples was determined using a Mann-Whitney two-tailed test. The sample size is indicated below each graph.

rhythm-generating network and rhythm generation does not require an alternating pattern of flexor-extensor activity. Our demonstration that IaINs and Renshaw cells are dispensable for rhythm generation also argues against half-center models that position IaINs and Renshaw cells at the center of a rhythm-generating network (Miller and Scott, 1977; Pratt and Jordan, 1987; Talpalar et al., 2011). Such models fail to account for the persistence of the motor rhythm when flexor-extensor alternation is disrupted (Figures 4 and 5), and they are difficult to reconcile with the more complex patterns of motor activity and resetting-deletions that occur during in vivo locomotion (McCrea and Rybak, 2008).

The pattern of locomotor activity produced by the *Gata3*^{Cre}; *En1*^{Cre}; *R26*$^{floxstop\text{-}TeNT}$ cord is consistent with a two-level CPG model that contains separate rhythm-generating level and pattern formation layers (McCrea and Rybak, 2008). In this configuration, V1 and V2b INs would be embedded in the pattern formation layer, where they would be a source of phasic inhibition to flexor and extensor motor neurons. They would also provide inhibitory feedback to the rhythm-generating layer to produce an alternating pattern of excitation to flexor and extensor motor neurons (Figure 9). Such a model is consistent with our demonstration that the flexor-extensor rhythm collapses into a single synchronous rhythm when V1- and V2b-derived inhibition is abrogated. This also leads us to speculate that the synchronous rhythmic activity seen in the *Gata3*^{Cre}; *En1*^{Cre}; *R26*$^{floxstop\text{-}TeNT}$ cord might be an atavistic rhythm, which is equivalent to a primitive swimming rhythm that lacks a differential flexor-extensor component. From an evolutionary perspective, this would provide a far more satisfactory solution to the issue of rhythm generation in limbed vertebrates than those presented by flexor-extensor half-center models.

Role of Ia Inhibitory INs in Flexor-Extensor Coordination

Our study leaves open the question as to whether flexor-extensor alternation is broadly encoded by the V1 and V2b populations as a whole or by the activity of specific V1 and V2b cell types, such as IaINs. The V1 and V2b IN classes are each composed of multiple cell types (Goulding, 2009). These include putative IaINs that constitute 29% and 19% of lumbar V1 and V2b cells, respectively. Renshaw cells make up a further 10%–12% of the V1 population (Sapir et al., 2004). The V1 and V2b IN classes are also likely to include other inhibitory subtypes with different connections and function. Consequently, caution needs to be exercised when ascribing the role of flexor-extensor coordination to a particular cell type, such as IaINs. Although IaINs possess the necessary attributes to play a prominent role in flexor-extensor control (Jankowska, 1992; Feldman and Orlovsky, 1975), their exact contribution to flexor-extensor alternation has yet to be determined. Our discovery that cells possessing the anatomical and functional features of IaINs arise from V1 and V2b INs (Figures 3 and 8) is consistent with a role for IaINs in flexor-extensor alternation. However, we currently lack the means to genetically isolate IaINs and evaluate their exact contribution to flexor-extensor motor behaviors. Furthermore, it is likely that flexor-extensor control, rather than being restricted to a dedicated physiological cell type, is instead distributed over multiple V1 and V2b cell types. In this respect, it is worth noting that fish with a primitive appendicular system

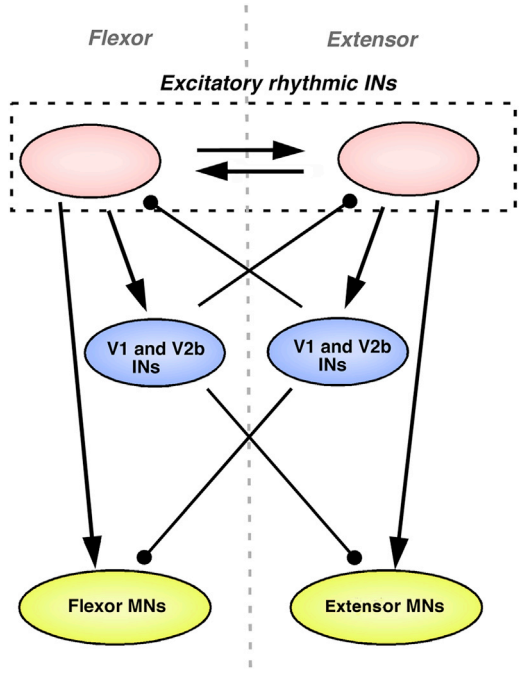

Figure 9. Model for V1 and V2b IN Control of Flexor-Extensor Motor Activity

Prospective model for how the limb CPG is functionally organized with respect to V1 and V2b INs. Arrows indicate excitatory pathways. Lines with filled spheres indicate inhibitory pathways. Weak excitatory connections between presumptive rhythm-generating excitatory neurons result in the synchronous rhythmic excitation of flexor and extensor motor neurons when V1 and V2b inhibition is absent.

do not possess specialized muscle spindles (Young, 1981), which is consistent with the idea that IaIN specialization occurred after the initial recruitment of V1 and V2b INs for flexor-extensor control.

Relationship of V1 and V2b INs to Spinal Neurons in Swimming Vertebrates

Our results reveal that the neurons mice use to secure alternating flexor-extensor driven limb movements share a common developmental origin with neurons that are part of the motor circuitry aquatic vertebrates use for swimming. The developmental homologs of V1 and V2b INs are present in the spinal cords of swimming vertebrates, with V2b INs being molecularly homologous to VeLD neurons (Batista et al., 2008; Peng et al., 2007) and V1 INs having as their homologs, aIN cells in *Xenopus* and CiA cells in zebrafish (Higashijima et al., 2004; Li et al., 2004). aIN and CiA inhibitory neurons are rhythmically active during swimming (Higashijima et al., 2004; Li et al., 2004), and they are candidates for the longitudinal inhibitory pathways that regulate intersegmental delay and the swim cycle period (Gabriel et al., 2008; Tegnér et al., 1993; Tunstall and Roberts, 1994). This leads us to posit that V1 and V2b INs were co-opted to produce an alternating motor output from motor neurons that innervate the fin adductor/abductor muscles in primitive fish.

In summary, this study provides evidence that the flexor-extensor system is organized around inhibitory V1 and V2b IN cell types, including IaINs, thereby demonstrating a developmental dichotomy in the composition of the spinal inhibitory network that secures flexor-extensor alternation in walking vertebrates. We would like to propose that the distribution of flexor-extensor control between V1 and V2b IN cell types arose as a result of the evolutionary reorganization of the swimming CPG circuit, and it was necessary for the emergence of movable bilateral appendages.

EXPERIMENTAL PROCEDURES

Animals

The generation, characterization, and genotyping of the *En1*^{Cre}, *Gata3*^{lacZ}, *Pax6*$^{-/-}$, *R26*$^{floxstop\text{-}lacZ}$, *R26*$^{floxstop\text{-}TeNT}$, *R26*$^{floxstop\text{-}GFP}$, *R26*$^{floxstop\text{-}Td\text{-}Tomato}$, *Gad1-GFP*, *GlyT2-GFP*, and *Thy1::floxstop-YFP* mice have been described previously (Buffelli et al., 2003; Gosgnach et al., 2006; Madisen et al., 2010; Stam et al., 2012; Tamamaki et al., 2003; van Doorninck et al., 1999; Zeilhofer et al., 2005; Zhang et al., 2008). Animal studies were approved by the Salk Animal Care and Use Committee and performed in accordance with the guidelines stipulated by the National Institutes of Health.

Generation of *Gata3*^{Cre} Mice

Sequences encoding for Cre recombinase and FRT-PGKneopA-FRT were inserted into the ATG of exon 2 of the *Gata3* gene by recombineering. 2A ES cells were electroporated with a linearized targeting vector and screened for homologous recombination. Two recombinant knockin cell lines gave germline transmission and the expected pattern of Cre recombination (see Figure S2).

In Situ Hybridization and Immunohistochemistry

X-gal staining, immunohistochemistry, and digoxigenin in situ hybridization analyses were performed using standard techniques (see Lanuza et al., 2004). In situ images were collected with a Zeiss Axioskop microscope using brightfield illumination. Fluorescence antibody stainings of spinal cord sections were imaged with Zeiss LSM510 and Olympus Fluoview 1000 confocal microscopes. All images were assembled using Photoshop software.

Retrograde Labeling of Neurons

Fluorescent Dextran Labeling

Fluorescent dextran labeling was performed as described previously (Sapir et al., 2004). Further details can be found online in the Supplemental Experimental Procedures.

Cholera Toxin-B Labeling of Motor Neurons

Individual muscles were injected unilaterally with Cy5-Cholera Toxin-B (CTB) as previously described by Shneider et al. (2009). Antibodies to the presynaptic markers vGAT and GlyT2 were used in combination with V1 and V2b IN-specific YFP reporters to visualize putative inhibitory synaptic contacts on Cy5-CTB-labeled motor neurons. Calbindin (Cb) immunohistochemistry was used to score Renshaw cell-derived contacts on motor neurons in the same pool.

Electrophysiology

Electroneurogram Recordings

Electrophysiological recordings were performed on embryonic E18.5 or postnatal P0 mice. Animals were anesthetized, decapitated, and spinal cords were dissected out in ice-cold Ringers solution. Ventral root electroneurogram (ENG) recordings were made as described previously (Lanuza et al., 2004). Rhythmic locomotor-like activity was induced either by adding NMDA (5 μM) and 5-hydroxytryptamine (5-HT; 15 μM) to the Ringer's perfusate or by electrical stimulation. For the latter, a train of 40 individual pulses (40–50 μA in amplitude and 500 μs in duration) were applied to the S1-S3 dorsal root on one side of the cord at 500 ms intervals. Signals were amplified, band-pass filtered, digitized, and collected with Axoscope and pCLAMP software.

Analysis of Locomotor Activity

Step cycle phase values (mean of 25–50 locomotor cycles) were calculated as described previously (Lanuza et al., 2004). Circular statistics (Zar, 1974) were used to determine the phasing and coupling strength between the L2, iL5, and cL2 ventral roots. Vector points (black dots) representing the mean phase values for 25–50 steps were determined for each cord. Angular vectors (blue arrows) illustrating the mean phase and concentration of phase values around the mean were then calculated for each experimental group.

Electromyogram Recordings

Electromyogram (EMG) recordings were performed on P0 mice. P0 pups were decapitated and dissected in ice-cold Ringer's solution. The cervical and thoracic spinal cord was exposed from the spinal column, while the trunk below diaphragm and hind legs being was kept intact. For recordings, two bipolar tungsten electrodes were inserted separately into thigh (Q) and posterior hamstring (PB/St) muscles. Locomotor activity was induced in the hindlimbs-attached preparation by adding NMDA (10 μM), 5-HT (25 μM), and dopamine (50 μM) to the Ringer's perfusate (Pearson et al., 2003). EMG signals were collected and filtered as described above for ventral root ENG recordings.

Intracellular Recordings of Muscle Afferent Input to Motor Neurons

The preparation used to assess the disynaptic inhibitory inputs from muscle afferents to motor neurons in neonate mice is shown schematically in Figure 8A. The methods used for recording and analyzing synaptic potentials are described in Wang et al. (2008). Positive current pulses (80–150 pA) were injected into some cells to depolarize them by 35–50 mV and test whether they are inhibitory, as assayed by the conversion of depolarizing synaptic potentials into hyperpolarizing potentials.

Tail Pinch Test

Behavioral tests were performed on awake P0 pups. Newborn pups were placed back down on a flat surface and the tail gently pinched by a pair of fine forceps. Each episode was video recorded, and the number of limb/torso movements for each episode was counted. Three replicates were performed for each pup.

Data Analysis and Statistical Tests

Circular statistics were used to evaluate the uniformity, quality, and coupling strength of ventral rooting activities as previously described (Lanuza et al., 2004; Zar, 1974). The angular value and step duration for each spinal cord was calculated for 25–50 cycles of locomotor activity. Rayleigh's test was performed to examine the uniformity within each group of spinal cord recordings. The difference of angular value between each group was examined by the Watson-William's test. Student's t test (with Bonferroni correction when needed), ANOVA, and Mann-Whitney tests were used for all other statistical analyses. p values less than 0.01 were considered highly significant.

SUPPLEMENTAL INFORMATION

Supplemental Information includes Supplemental Experimental Procedures, six figures, and one table and can be found with this article online at http://dx.doi.org/10.1016/j.neuron.2014.02.013.

AUTHOR CONTRIBUTIONS

Jingming Zhang undertook all of the electrophysiological analyses. The recordings in Figure 8 were performed by Zhi Wang, with help from Jingming Zhang. Guillermo Lanuza generated and characterized the *Gata3*^{Cre} knockin mice used in this study. He also performed the anatomical and neurotracing analyses with help from Valerie Seimbab. Both co-first authors helped with the experimental design and writing of the manuscript.

ACKNOWLEDGMENTS

We would like to thank Simon Gosgnach for his early contribution to the analysis of the *Pax6* mutant mice. We also thank Tom Jessell, Chris Kintner, Greg Lemke, John Thomas, Lidia Garcia-Campmany, and James Flynn for their thoughtful comments and criticisms. This research was supported by grants from the National Institutes of Health (R37-NS037075, P01-NS031249, R01-NS080586, and R01-NS047357), the Human Frontier Science Program, and the Christopher and Dana Reeve Foundation. G.M.L. was supported by an HFSP postdoctoral fellowship.

Accepted: January 24, 2014
Published: April 2, 2014

REFERENCES

Al-Mosawie, A., Wilson, J.M., and Brownstone, R.M. (2007). Heterogeneity of V2-derived interneurons in the adult mouse spinal cord. Eur. J. Neurosci. *26*, 3003–3015.

Alvarez, F.J., Jonas, P.C., Sapir, T., Hartley, R., Berrocal, M.C., Geiman, E.J., Todd, A.J., and Goulding, M. (2005). Postnatal phenotype and localization of spinal cord V1 derived interneurons. J. Comp. Neurol. *493*, 177–192.

Andersson, L.S., Larhammer, M., Memic, F., Wootz, H., Schwochow, D., Rubin, C.-J., Patra, K., Arnason, T., Wellbring, L., Hjalm, G., et al. (2012). Mutations in DMRT3 affect locomotion in horses and spinal cord circuit function in mice. Nature *488*, 642–647.

Batista, M.F., Jacobstein, J., and Lewis, K.E. (2008). Zebrafish V2 cells develop into excitatory CiD and Notch signalling dependent inhibitory VeLD interneurons. Dev. Biol. *322*, 263–275.

Betley, J.N., Wright, C.V., Kawaguchi, Y., Erdélyi, F., Szabó, G., Jessell, T.M., and Kaltschmidt, J.A. (2009). Stringent specificity in the construction of a GABAergic presynaptic inhibitory circuit. Cell *139*, 161–174.

Bracci, E., Ballerini, L., and Nistri, A. (1996). Localization of rhythmogenic networks responsible for spontaneous bursts induced by strychnine and bicuculline in the rat isolated spinal cord. J. Neurosci. *16*, 7063–7076.

Brown, T.G. (1911). The intrinsic factors in the act of progression in the mammal. Proc. Royal Acad. Sci. *84*, 308–319.

Buffelli, M., Burgess, R.W., Feng, G., Lobe, C.G., Lichtman, J.W., and Sanes, J.R. (2003). Genetic evidence that relative synaptic efficacy biases the outcome of synaptic competition. Nature *424*, 430–434.

Cazalets, J.-R., Bertrand, S., Sqalli-Houssaini, Y., and Clarac, F. (1998). GABAergic control of spinal locomotor networks in the neonatal rat. Ann. N Y Acad. Sci. *860*, 168–180.

Cowley, K.C., and Schmidt, B.J. (1995). Effects of inhibitory amino acid antagonists on reciprocal inhibitory interactions during rhythmic motor activity in the in vitro neonatal rat spinal cord. J. Neurophysiol. *74*, 1109–1117.

Cowley, K.C., Zaporozhets, E., Maclean, J.N., and Schmidt, B.J. (2005). Is NMDA receptor activation essential for the production of locomotor-like activity in the neonatal rat spinal cord? J. Neurophysiol. *94*, 3805–3814.

Crone, S.A., Quinlan, K.A., Zagoraiou, L., Droho, S., Restrepo, C.E., Lundfald, L., Endo, T., Setlak, J., Jessell, T.M., Kiehn, O., and Sharma, K. (2008). Genetic ablation of V2a ipsilateral interneurons disrupts left-right locomotor coordination in mammalian spinal cord. Neuron *60*, 70–83.

Eccles, J.C., Fatt, P., and Landgren, S. (1956). Central pathway for direct inhibitory action of impulses in largest afferent nerve fibres to muscle. J. Neurophysiol. *19*, 75–98.

Ericson, J., Rashbass, P., Schedl, A., Brenner-Morton, S., Kawakami, A., van Heyningen, V., Jessell, T.M., and Briscoe, J. (1997). Pax6 controls progenitor cell identity and neuronal fate in response to graded Shh signaling. Cell *90*, 169–180.

Feldman, A.G., and Orlovsky, G.N. (1975). Activity of interneurons mediating reciprocal 1a inhibition during locomotion. Brain Res. *84*, 181–194.

Gabriel, J.P., Mahmood, R., Walter, A.M., Kyriakatos, A., Hauptmann, G., Calabrese, R.L., and El Manira, A. (2008). Locomotor pattern in the adult zebrafish spinal cord in vitro. J. Neurophysiol. *99*, 37–48.

Gosgnach, S., Lanuza, G.M., Butt, S.J., Saueressig, H., Zhang, Y., Velasquez, T., Riethmacher, D., Callaway, E.M., Kiehn, O., and Goulding, M. (2006). V1

spinal neurons regulate the speed of vertebrate locomotor outputs. Nature *440*, 215–219.

Goulding, M. (2009). Circuits controlling vertebrate locomotion: moving in a new direction. Nat. Rev. Neurosci. *10*, 507–518.

Grillner, S. (1975). Locomotion in vertebrates: central mechanisms and reflex interaction. Physiol. Rev. *55*, 247–304.

Grillner, S., and Jessell, T.M. (2009). Measured motion: searching for simplicity in spinal locomotor networks. Curr. Opin. Neurobiol. *19*, 572–586.

Gross, M.K., Dottori, M., and Goulding, M. (2002). Lbx1 specifies somatosensry association neurons in the dorsal spinal cord. Neuron *34*, 1–20.

Harrison, P.J., Jankowska, E., and Zytnicki, D. (1986). Lamina VIII interneurones interposed in crossed reflex pathways in the cat. J. Physiol. *371*, 147–166.

Higashijima, S., Masino, M.A., Mandel, G., and Fetcho, J.R. (2004). Engrailed-1 expression marks a primitive class of inhibitory spinal interneuron. J. Neurosci. *24*, 5827–5839.

Hultborn, H., Jankowska, E., and Lindström, S. (1971). Recurrent inhibition of interneurones monosynaptically activated from group Ia afferents. J. Physiol. *215*, 613–636.

Jankowska, E. (1992). Interneuronal relay in spinal pathways from proprioceptors. Prog. Neurobiol. *38*, 335–378.

Jankowska, E., and Lindström, S. (1972). Morphology of interneurones mediating Ia reciprocal inhibition of motoneurones in the spinal cord of the cat. J. Physiol. *226*, 805–823.

Jankowska, E., and Roberts, W.J. (1972). Synaptic actions of single interneurones mediating reciprocal Ia inhibition of motoneurones. J. Physiol. *222*, 623–642.

Kiehn, O. (2006). Locomotor circuits in the mammalian spinal cord. Annu. Rev. Neurosci. *29*, 279–306.

Kremer, E., and Lev-Tov, A. (1997). Localization of the spinal network associated with generation of hindlimb locomotion in the neonatal rat and organization of its transverse coupling system. J. Neurophysiol. *77*, 1155–1170.

Ladle, D.R., Pecho-Vrieseling, E., and Arber, S. (2007). Assembly of motor circuits in the spinal cord: driven to function by genetic and experience-dependent mechanisms. Neuron *56*, 270–283.

Lanuza, G.M., Gosgnach, S., Pierani, A., Jessell, T.M., and Goulding, M. (2004). Genetic identification of spinal interneurons that coordinate left-right locomotor activity necessary for walking movements. Neuron *42*, 375–386.

Li, W.C., Higashijima, S., Parry, D.M., Roberts, A., and Soffe, S.R. (2004). Primitive roles for inhibitory interneurons in developing frog spinal cord. J. Neurosci. *24*, 5840–5848.

Lundfald, L., Restrepo, C.E., Butt, S.J., Peng, C.-Y., Droho, S., Endo, T., Zeilhofer, H.U., Sharma, K., and Kiehn, O. (2007). Phenotype of V2-derived interneurons and their relationship to the axon guidance molecule EphA4 in the developing mouse spinal cord. Eur. J. Neurosci. *26*, 2989–3002.

Madisen, L., Zwingman, T.A., Sunkin, S.M., Oh, S.W., Zariwala, H.A., Gu, H., Ng, L.L., Palmiter, R.D., Hawrylycz, M.J., Jones, A.R., et al. (2010). A robust and high-throughput Cre reporting and characterization system for the whole mouse brain. Nat. Neurosci. *13*, 133–140.

McCrea, D.A., and Rybak, I.A. (2008). Organization of mammalian locomotor rhythm and pattern generation. Brain Res. Brain Res. Rev. *57*, 134–146.

Miller, S., and Scott, P.D. (1977). The spinal locomotor generator. Exp. Brain Res. *30*, 387–403.

Ornung, G., Ottersen, O.P., Cullheim, S., and Ulfhake, B. (1998). Distribution of glutamate-, glycine- and GABA-immunoreactive nerve terminals on dendrites in the cat spinal motor nucleus. Exp. Brain Res. *118*, 517–532.

Pearson, S.A., Mouihate, A., Pittman, Q.J., and Whelan, P.J. (2003). Peptidergic activation of locomotor pattern generators in the neonatal spinal cord. J. Neurosci. *23*, 10154–10163.

Peng, C.-Y., Yajima, H., Burns, C.E., Zon, L.I., Sisodia, S.S., Pfaff, S.L., and Sharma, K. (2007). Notch and MAML signaling drives Scl-dependent interneuron diversity in the spinal cord. Neuron *53*, 813–827.

Pratt, C.A., and Jordan, L.M. (1987). Ia inhibitory interneurons and Renshaw cells as contributors to the spinal mechanisms of fictive locomotion. J. Neurophysiol. *57*, 56–71.

Sapir, T., Geiman, E.J., Wang, Z., Velasquez, T., Mitsui, S., Yoshihara, Y., Frank, E., Alvarez, F.J., and Goulding, M. (2004). *Pax6* and *Engrailed 1* regulate two distinct aspects of Renshaw cell development. J. Neurosci. *24*, 1255–1264.

Saueressig, H., Burrill, J., and Goulding, M. (1999). Engrailed-1 and netrin-1 regulate axon pathfinding by association interneurons that project to motor neurons. Development *126*, 4201–4212.

Sernagor, E., Chub, N., Ritter, A., and O'Donovan, M.J. (1995). Pharmacological characterization of the rhythmic synaptic drive onto lumbosacral motoneurons in the chick embryo spinal cord. J. Neurosci. *15*, 7452–7464.

Sherrington, C.S. (1893). Further experimental note on the correlation of action of antagonistic muscles. BMJ *1*, 1218.

Shigenaga, Y., Moritani, M., Oh, S.J., Park, K.P., Paik, S.K., Bae, J.Y., Kim, H.N., Ma, S.K., Park, C.W., Yoshida, A., et al. (2005). The distribution of inhibitory and excitatory synapses on single, reconstructed jaw-opening motoneurons in the cat. Neuroscience *133*, 507–518.

Shneider, N.A., Mentis, G.Z., Schustak, J., and O'Donovan, M.J. (2009). Functionally reduced sensorimotor connections form with normal specificity despite abnormal muscle spindle development: the role of spindle-derived neurotrophin 3. J. Neurosci. *29*, 4719–4735.

Stam, F.J., Hendricks, T.J., Zhang, J., Geiman, E.J., Francius, C., Labosky, P.A., Clotman, F., and Goulding, M. (2012). Renshaw cell interneuron specialization is controlled by a temporally restricted transcription factor program. Development *139*, 179–190.

Stepien, A.E., and Arber, S. (2008). Probing the locomotor conundrum: descending the 'V' interneuron ladder. Neuron *60*, 1–4.

Stepien, A.E., Tripodi, M., and Arber, S. (2010). Monosynaptic rabies virus reveals premotor network organization and synaptic specificity of cholinergic partition cells. Neuron *68*, 456–472.

Talpalar, A.E., Endo, T., Löw, P., Borgius, L., Hägglund, M., Dougherty, K.J., Ryge, J., Hnasko, T.S., and Kiehn, O. (2011). Identification of minimal neuronal networks involved in flexor-extensor alternation in the mammalian spinal cord. Neuron *71*, 1071–1084.

Talpalar, A.E., Bouvier, J., Borgius, L., Fortin, G., Pierani, A., and Kiehn, O. (2013). Dual-mode operation of neuronal networks involved in left-right alternation. Nature *500*, 85–88.

Tamamaki, N., Yanagawa, Y., Tomioka, R., Miyazaki, J., Obata, K., and Kaneko, T. (2003). Green fluorescent protein expression and colocalization with calretinin, parvalbumin, and somatostatin in the GAD67-GFP knock-in mouse. J. Comp. Neurol. *467*, 60–79.

Tegnér, J., Matsushima, T., el Manira, A., and Grillner, S. (1993). The spinal GABA system modulates burst frequency and intersegmental coordination in the lamprey: differential effects of $GABA_A$ and $GABA_B$ receptors. J. Neurophysiol. *69*, 647–657.

Tripodi, M., Stepien, A.E., and Arber, S. (2011). Motor antagonism exposed by spatial segregation and timing of neurogenesis. Nature *479*, 61–66.

Tunstall, M.J., and Roberts, A. (1994). A longitudinal gradient of synaptic drive in the spinal cord of Xenopus embryos and its role in co-ordination of swimming. J. Physiol. *474*, 393–405.

van Doorninck, J.H., van Der Wees, J., Karis, A., Goedknegt, E., Engel, J.D., Coesmans, M., Rutteman, M., Grosveld, F., and De Zeeuw, C.I. (1999). GATA-3 is involved in the development of serotonergic neurons in the caudal raphe nuclei. J. Neurosci. *19*, RC12.

Wang, Z., Li, L., Goulding, M., and Frank, E. (2008). Early postnatal development of reciprocal Ia inhibition in the murine spinal cord. J. Neurophysiol. *100*, 185–196.

Whelan, P., Bonnot, A., and O'Donovan, M.J. (2000). Properties of rhythmic activity generated by the isolated spinal cord of the neonatal mouse. J. Neurophysiol. *84*, 2821–2833.

Wilson, J.M., Blagovechtchenski, E., and Brownstone, R.M. (2010). Genetically defined inhibitory neurons in the mouse spinal cord dorsal horn: a possible source of rhythmic inhibition of motoneurons during fictive locomotion. J. Neurosci. *30*, 1137–1148.

Young, J.Z. (1981). The Life of Vertebrates, Third Edition. (Oxford: Oxford University Press).

Zagoraiou, L., Akay, T., Martin, J.F., Brownstone, R.M., Jessell, T.M., and Miles, G.B. (2009). A cluster of cholinergic premotor interneurons modulates mouse locomotor activity. Neuron *64*, 645–662.

Zar, J.H. (1974). Biostatistical Analysis. (Engelwood Cliffs, NJ: Prentice Hall).

Zeilhofer, H.U., Studler, B., Arabadzisz, D., Schweizer, C., Ahmadi, S., Layh, B., Bösl, M.R., and Fritschy, J.M. (2005). Glycinergic neurons expressing enhanced green fluorescent protein in bacterial artificial chromosome transgenic mice. J. Comp. Neurol. *482*, 123–141.

Zhang, Y., Narayan, S., Geiman, E., Lanuza, G.M., Velasquez, T., Shanks, B., Akay, T., Dyck, J., Pearson, K., Gosgnach, S., et al. (2008). V3 spinal neurons establish a robust and balanced locomotor rhythm during walking. Neuron *60*, 84–96.